Sonoluminescence radiation from different concentrations of sulfuric acid

A. Moshaii,[1,*] Kh. Imani,[2] and M. Silatani[2]
[1]*Department of Physics, Tarbiat Modares University, P.O. Box 14115-175, Tehran, Iran*
[2]*Department of Physics, Sharif University of Technology, P.O. Box 11365-9567, Tehran, Iran*
(Received 22 January 2009; revised manuscript received 17 August 2009; published 30 October 2009)

Sonoluminescence (SL) radiation from an argon bubble in water and in different concentrations of sulfuric acid has numerically been studied to quantify the effects of vapor pressure and viscosity of the liquid on cavitation luminescence in a liquid with controllable vapor pressure and viscosity. For the solutions containing the noble gas with low partial pressure (about 4 Torr), it is shown that there exists an optimum acid solution in which both the temperature and the intensity of SL radiation become maximum. The calculations show that the maximum SL radiation is achieved from the solution of around 65% (wt.) H_2SO_4, which is in agreement with available experimental results.

DOI: 10.1103/PhysRevE.80.046325 PACS number(s): 78.60.Mq

Single-bubble sonoluminescence (SL) is the production of periodic picosecond light pulses from the sound waves concentrated inside a collapsing bubble [1–3]. The spectrum of such radiation is usually continuum, extending from 200 to 800 nm with increment toward ultraviolet region [4]. The fitting of SL spectrum with black-body radiation indicates the emission is originated from an optically transparent spherical shell inside the bubble in which the temperature is about 6000–20 000 K [5,6]. The spherical shell seems to include a very hot opaque plasma with the temperature more than 1 million Kelvin [7]. On the other hand, when the SL bubble is driven with lower pressure amplitudes of the pressure domain of SL, which corresponds to SL emission with lower intensities, a number of atomic, ionic, and molecular spectral lines appear in the SL spectrum with the spectroscopic temperatures in the range of 4000–15 000 K [8–13].

In the high-temperature region attainable at the collapse, the liquid molecules evaporated from the bubble wall are chemically dissociated by usually endothermic reactions [14,15]. The chemical reactions consume a considerable part of the bubble thermal energy and limit the peak temperature attainable at the collapse. Therefore, to generate SL with higher temperatures and higher intensities, the surrounding liquid should be chosen from the liquids with enough low vapor pressure such as sulfuric and phosphoric acids [13,16]. Experiments show that the intensity of SL radiation in sulfuric acid is about three orders of magnitude greater than the radiation from a standard SL bubble in water [13,17].

In spite of the considerable improvement of SL intensity in liquids with low vapor pressure, it seems that the effect of vapor pressure is not just limited to diminishing the SL intensity. The production of SL in different concentrations of sulfuric acid indicates there exits an optimum acid concentration (about 50 vol. %) for creating the highest SL radiation [18]. Since the vapor pressure of a sulfuric acid solution monotonically decreases with the acid concentration, the SL radiation is expected to be maximum in a solution close to 100% acid not in a moderate acid concentration.

On the other hand, the increment of liquid-vapor pressure increases the number of particles inside the bubble. Since, during the collapse of bubble, all of the vapor molecules are not condensed on the bubble wall, therefore, a fraction of these vapor molecules remain inside the bubble at the time of SL emission. This means that the total number of particles inside the bubble at the end of collapse can be greater for a liquid with higher vapor pressure. In this case, if for the liquid with higher vapor pressure, the instability mechanisms let the bubble to be driven with a more intense collapse, then the bubble can get a higher compression at the collapse and reaches to a higher temperature.

To numerically examine the optimum concentration of sulfuric acid for acquiring the most compression inside the bubble and getting the maximum SL temperature, all the effects arising from the change in acid concentration must be considered in the description of the bubble oscillations. With the change in concentration of sulfuric acid, the physical parameters of the liquid surrounding the bubble change. This not only changes the number of particles inside the bubble but also changes the phase diagrams of the bubble oscillations. By calculating the maximum SL emission from different concentrations of sulfuric acid, we show there exists an optimum acid concentration in which the SL radiation gets its maximum intensity. We also show that the optimum concentration is mainly determined by an increment of viscosity of the acid with its concentration and the change in vapor pressure of the acid is not so important.

To quantitatively clarify the influence of vapor pressure and viscosity on SL intensity, we have calculated the production of SL in different concentrations of sulfuric acid in which the vapor pressure changes over three orders of magnitude. The performed simulation is based on a hydrochemical model considering the bubble inside as a uniform medium [19,20]. The bubble dynamic is described by the Rayleigh-Plesset (RP) equation [21] along with van der Waals equation as the equation of state

$$\left(1-\frac{\dot{R}}{C}\right)R\ddot{R}+\frac{3}{2}\left(1-\frac{\dot{R}}{3C}\right)\dot{R}^2 = \frac{R}{\rho C}\frac{d}{dt}(P_l-P_a)+\left(1+\frac{\dot{R}}{C}\right)\frac{P_l-P_a-P_0}{\rho},$$

*moshaii@modares.ac.ir

TABLE I. Physical parameters of water and four different concentrations of sulfuric acid at room temperature, which are used in the simulation [29].

Sulfuric acid concentration (wt %)	85	70	65	45	Water
P_{H_2O}(Pa)	2.45	99.5	233.2	1170	2064
$P_{H_2SO_4}(10^{-7}$ Pa)	1790	6.49	3.32	2.2	0
ρ(Kg/m^3)	1778.6	1633.8	1531.0	1347.6	998
μ(mPa)	25.08	13.08	6.9	3.18	1
$\sigma(\times 10^{-3}$ N/m)	56.025	61.020	62.91	70.344	70.7
C(m/s)	1645	1638	1631	1640	1483

$$P_l = P_g - 4\frac{\mu\dot{R}}{R} - 2\frac{\sigma}{R}, \quad P_g = \frac{N_{tot}kT_g}{V - N_{tot}B},$$

where R is the bubble radius, C and ρ are velocity of sound and density of surrounding liquid, P_0 and P_a are ambient and deriving pressures, and P_l and P_g are liquid and gas pressures at the bubble interface, respectively. Also, μ, N_{tot}, and T_g are liquid coefficient of viscosity, total number of particles inside the bubble, and gas temperature, respectively. The hard-core parameter $B=5.1\times10^{-29}$ m^3 is assumed to be equal for all particles [19].

At the beginning of each period, the bubble's contents are argon, water vapor, and sulfuric acid molecules. Due to dissociations of water vapor at the collapse, five more chemical radicals and molecules are created inside the bubble; H, H_2, OH, O, and O_2. The rate of a chemical reaction is calculated by the Arrhenius laws. We used the scheme of Ref. [19] to consider eight chemical reactions occurring inside the bubble due to the dissociation of water vapor molecules. The dissociation of sulfuric acid molecules is neglected due to the smallness of partial vapor pressure of sulfuric acid relative to water in all sulfuric acid solutions (see Table I). The diffusion of chemical reaction products from the bubble to the surrounding liquid is considered by the boundary layer formalism of Ref. [22]

$$\dot{N}_i^d = -4\pi R^2 D\frac{n_i}{l_d}, \quad l_d = \min\left(\sqrt{\frac{RD}{|\dot{R}|}}, \frac{R}{\pi}\right), \tag{1}$$

where $\dot{N}_i^d$ and n_i are the diffusion rate and the instantaneous concentration of particle species i. The coefficient D is the diffusion coefficient given by $D=D_0(n_0/n_{tot})$, where $D_0=23.55\times10^{-6}$ m^2/s [19] and n_{tot} is the instantaneous total number density of the bubble and n_0 is the value of n_{tot} at the beginning of the bubble evolution. The quantity l_d is the thickness of the diffusive boundary layer.

We also used the boundary layer formalism to consider heat transfer between the bubble and its surrounding liquid [22]

$$\dot{Q} = 4\pi R^2\kappa\frac{T_0 - T_g}{l_{th}}, \quad l_{th} = \min\left(\sqrt{\frac{R\chi}{|\dot{R}|}}, \frac{R}{\pi}\right), \tag{2}$$

where $\dot{Q}$ is the rate of heat transfer at the bubble wall and κ is the thermal-conductivity coefficient of the gas inside the bubble. l_{th} is the thickness of thermal boundary layer and χ is the thermal diffusivity coefficient of the bubble content given by $\chi=\kappa/c_p$, with c_p as the constant pressure heat capacity of the bubble contents [19]. Also, T_0 is the ambient temperature. The model includes variation in thermal conductivity of the gas with temperature up to 2500 K by a quadratic polynomial formula introduced by Ho *et al.* [23], as used in Ref. [24].

One of the characteristics of this simulation relative to other studies [25,26] is the consideration of evaporation and condensation of water vapor and sulfuric acid molecules at the bubble interface. The number of vapor molecules of particle species i inside the bubble is determined from its corresponding partial vapor pressure in the acid solution as [27,28]

$$\dot{N}_i = 4\pi R^2 J_i,$$

$$J_i = \frac{\alpha_M}{\sqrt{2\pi M_i k_B/N_A}}\left(\frac{P_i^{vap}}{\sqrt{T_0}} - \frac{\Gamma_i P_i}{\sqrt{T_g}}\right), \tag{3}$$

where $\dot{N}_i$ is the rate of change in vapor species i with the molar mass M_i. Also, J_i is the rate of flow of vapor molecules at the bubble wall. P_i is the instantaneous partial pressure inside the bubble and P_i^{vap} is the equilibrium vapor pressure at the ambient temperature T_0. k_B and N_A are the Boltzmann's constant and Avogadro's number, respectively. The index i is used for water vapor and sulfuric acid molecules, separately. Also, $\alpha_M=0.35$ is the accommodation coefficient for vapor molecules at the bubble surface (assumed the same for both water and sulfuric acid). The correction factor Γ_i is calculated from [28]

$$\Gamma_i = \exp(\Omega_i^2) - \Omega_i\sqrt{\pi}[1 - \mathrm{erf}(\Omega_i)], \tag{4}$$

in which

$$\Omega_i = \frac{J_i}{P_i}\sqrt{\frac{N_A k_B T_g}{2M_i}}. \tag{5}$$

The values of the partial vapor pressure of water and sulfuric acid in different acid concentrations in addition to the other physical parameters used in the simulation are listed in Table I.

Time evolution of the gas temperature is calculated from the energy equation of the bubble content [22]

TABLE II. Characteristic vibrational temperatures (in K) of various particles considered in the hydrochemical model and their numbers of translational+rotational degree of freedom f [30].

Species	H_2SO_2	H_2O	O_2	H_2	OH	O	H	Ar
f	6	6	5	5	5	3	3	3
Θ_1	322.0	2295	2273	6325	5370			
Θ_2	414.0	5255						
Θ_3	545.0	5400						
Θ_4	607.0							
Θ_5	728.0							
Θ_6	789.0							
Θ_7	803.0							
Θ_8	1196.0							
Θ_9	1269.0							
Θ_{10}	1635.0							
Θ_{11}	1665.0							
Θ_{12}	1750.0							
Θ_{13}	2090.0							
Θ_{14}	5128.0							
Θ_{15}	5133.0							

$$\dot{T}_g \frac{\partial e_{th,j}}{\partial T_g} N_j = \dot{Q} - P_g \dot{V} - \sum_j e_{th,j} \dot{N}_j + \dot{E}_{chem} + \sum_j h_{w,j} \dot{N}_j^d, \tag{6}$$

where $h_{w,j}=(1+f_j/2)kT_0$ is the molecular enthalpy of the particle species j at the bubble wall temperature T_0, with f_j as its number of translational+rotational degree of freedom. The quantity $\dot{E}_{chem}$ denotes the rate of change in the chemical energy of the bubble due to eight chemical reactions considered in the model [19]. Also, $e_{th,j}$ is the thermal energy of the molecule j given by

$$e_{th,j} = \frac{f_j}{2} kT_g + \sum_l \frac{k\Theta_{j,l}}{e^{(\Theta_{j,l}/T_g)} - 1}, \tag{7}$$

with $\Theta_{j,l}$ as the various characteristic vibrational temperatures of the particle species j. Table II lists the characteristic vibrational temperatures of various particles considered in the model along with the values of factor f for these particles.

Equations (1)–(7) along with the RP and van der Waals equations are the set of equations which totally describe the evolution of the SL bubble.

To have stable oscillations for a long time, the SL bubble should be stable under the influences of three major instabilities; i.e., shape, diffusion, and positional instabilities [15]. The schemes of considering shape and diffusion instabilities in the model are the same as those of Ref. [19], which are not repeated here again.

The threshold of positional instability is determined from calculating primary Bjerknes force acting on the bubble [31]

$$\mathbf{F}_B = f_B \mathbf{r}, \quad f_B = \frac{4}{9} \pi k^2 \langle R^3(t) p_a(t) \rangle, \tag{8}$$

where $\langle \ldots \rangle$ denotes time averaging over one period of the ultrasound field and r is the radial displacement of the bubble from the pressure antinode of the acoustic field. Also, $p_a=-P_a \sin(\omega t)$ is the acoustic pressure at the bubble equilibrium position, with ω and $k=\omega/C$ as the frequency and the wave number of the sound field. Equation (8) is valid for a spherical resonator as an approximation of the Bessel function, which is the solution of the linear wave equation in spherical geometry [31].

The quantity f_B in Eq. (8) is equivalent to the stiffness coefficient for springlike modeling of the bubble displacement [31]. If f_B is negative, the primary Bjerknes force is directed toward the bubble equilibrium position, and the bubble is positionally stable. If $f_B>0$, the bubble is repelled from the pressure antinode and is positionally unstable.

The phase diagram of the SL bubble can be calculated from the stability scheme of the model. Figure 1 shows the calculated phase diagrams in different concentrations of sulfuric acid containing argon at partial pressures of 4 and 50 Torr. As the concentration of the acid increases, the phase parameters corresponding to a stable SL bubble shift toward higher-pressure amplitudes. Also, with increment of the acid concentration, the capability of Bjerkness force acting on the bubble to keep the bubble stable at its equilibrium position decreases. In fact, in concentrated acid solutions, the positional instability is the dominant instability determining the ultimate driving parameters for the stable SL bubble. This result is in good agreement with experimental reports [13,18]. As shown in Fig. 1, the positional instability is the dominant instability for the concentration of 85% sulfuric acid and for partial pressure of 4 Torr in the concentration of 65% acid. For all other solutions, the dominant instability is the shape instability.

The driving parameters for acquiring maximum SL radiation in each acid solution of Fig. 1 are determined from the

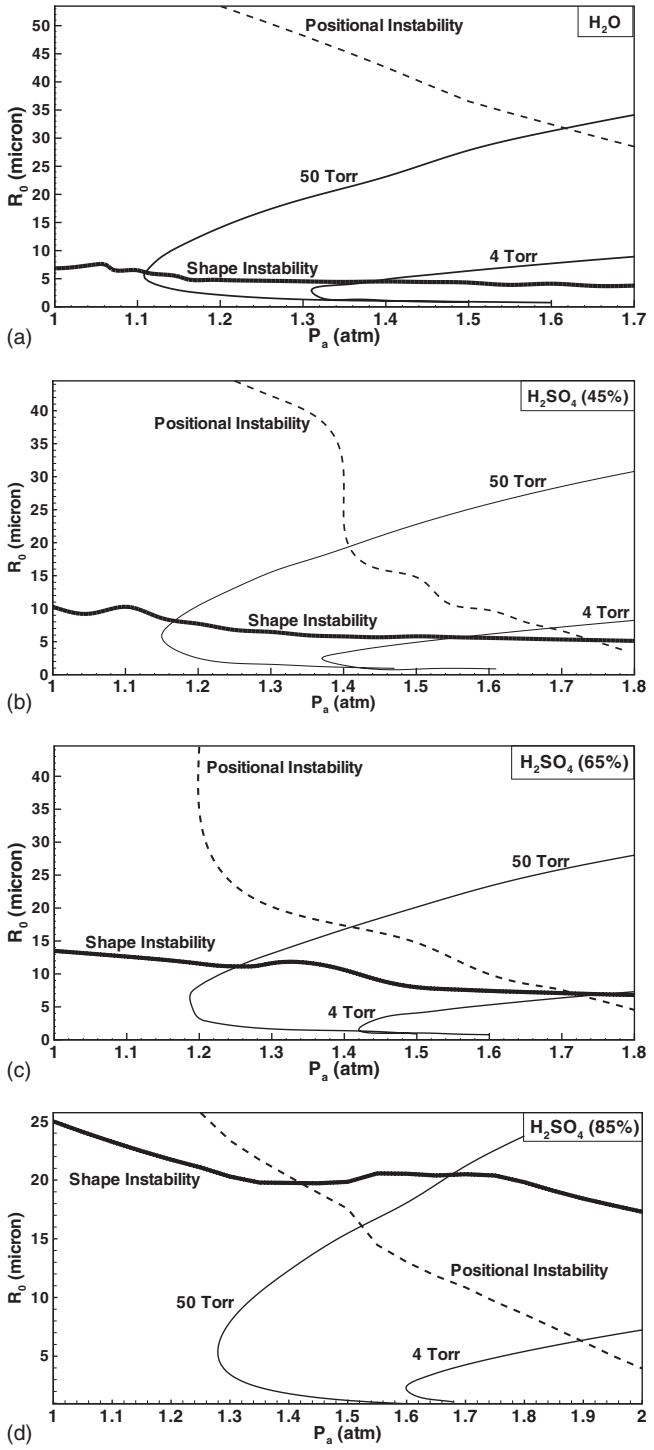

FIG. 1. Phase diagrams of sonoluminescence for water and three different concentrations of sulfuric acid containing argon at partial pressures 4 and 50 Torr. The driving parameters for the SL bubble are ν=38.0 KHz, P_0=1.0 atm, and T_0=273.13 K.

phase parameters of the point of crossing of diffusion stability curve with the dominant instability curve of that solution. Figure 2 shows time evolution of the bubble characteristics for the conditions of maximum SL radiation from various acid solutions containing argon at partial pressure 4 Torr. It is seen that with an increment of the acid concentration, the collapse of bubble shifts toward the compression phase of

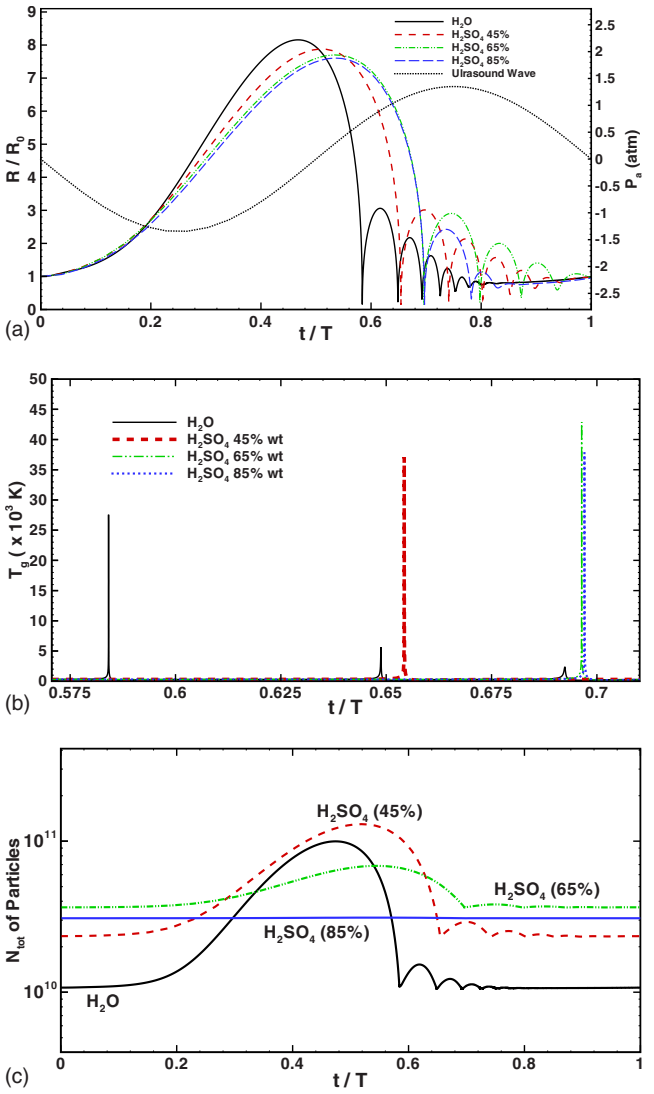

FIG. 2. (Color online) Bubble characteristics as a function of time for water and three different concentrations of sulfuric acid containing argon at partial pressure 4 Torr: (a) normalized bubble radius, (b) bubble temperature, and (c) the number of particles inside the bubble. The driving pressure for each solution is obtained from the cross point of diffusion stability curve with the dominant instability for that solution in Fig. 1. The time in all graphs has been normalized by the period of the ultrasound field T.

the ultrasound field. This change is more significant for lower acid concentrations. Details of our calculations in Fig. 2(b) show that among the different acid concentrations, the solution of 65% acid has the most SL temperature. Moreover, we show later that for the partial pressure 4 Torr, the SL intensity is also maximum for the solution of 65% acid.

From Fig. 2(c), it is seen that the bubble in the solution of 65% acid also has the most number of particles at the end of collapse. Details of our calculations in Table III show that both of the quantities of maximum gas pressure and maximum number density of the bubble $[n_{tot}=N_{tot}/(V-BN_{tot})]$ get their greatest values in the case of 65% acid, showing that the biggest compression is reached in this case. It should be mentioned that due to a large amount of evaporation and condensation of vapor molecules occurring inside the SL

TABLE III. The values of bubble characteristics at the time of maximum SL emission from water and four different concentrations of sulfuric acid. The results are for partial pressures of 4 and 50 Torr of the noble gas. In both cases, the radiation intensity has been normalized to the maximum acquirable SL intensity in that case.

Sulfuric acid concentration (wt %)	85	70	65	45	0 (Water)
			4 Torr		
P_a(atm)	1.89	1.78	1.73	1.60	1.37
$R_0(\mu m)$	6.31	6.52	6.65	5.65	4.26
R_{max}/R_0	7.606	7.663	7.701	7.879	8.156
R_0/R_{min}	6.884	6.885	6.905	6.816	6.495
R_{max}/R_{min}	52.36	52.76	53.18	53.70	52.97
$T_{g_{max}}$(K)	37998	41305	43202	37749	27564
$P_{g_{max}}$(atm)	97067	107318	114749	103051	68311
$n_{tot_{max}}(10^{28}\ m^{-3})$	1.874	1.910	1.959	2.0619	1.818
Relative intensity	0.44	0.76	1.0	0.37	0.024
			50 Torr		
P_a(atm)	1.523	1.35	1.253	1.116	1.11
$R_0(\mu m)$	16.13	13.33	11.13	7.81	6.12
R_{max}/R_0	3.233	3.316	3.374	3.520	3.654
R_0/R_{min}	4.127	4.191	4.246	4.109	3.833
R_{max}/R_{min}	13.34	13.90	13.33	14.46	14.01
$T_{g_{max}}$(K)	7353	7096	6648	5253	4210
$P_{g_{max}}$(atm)	2056	2159	2156	1614	1068
$n_{tot_{max}}(10^{27}\ m^{-3})$	2.052	2.232	2.380	2.255	1.861
Relative intensity	1.0	0.34	0.008	4.6E-4	2.2E-6

bubble in water, the number of particles in this case changes more than one order of magnitude in a period, while, the number of particles in the bubble of 85% acid does not practically change during a period (less than 1.0%) and the bubble is fully occupied by the noble gas atoms.

Since both of the SL temperature and the number of particles inside the bubble get their maximums in the solution of 65% acid, then the SL intensity is expected to be maximum in this solution. By calculating the SL intensity from the model of Yasui [32], the results of simulation can be compared with available experimental data from Ref. [18] shown in Fig. 3. We see a good agreement between the experimental and the simulation results, where in both cases the SL intensity is maximum for the solution of 65% (wt.) sulfuric acid, which is equivalent to the volume concentration of 50% acid presented in [18].

The importance of SL production in liquids with low partial pressures of noble gases is in getting higher SL temperatures from the liquids with the lower amount of dissolved noble gases. As shown in Fig. 1, reducing the partial pressure of the noble gas in the liquid decreases the size of SL bubble and shifts the domain of driving pressure toward higher-pressure amplitudes. Therefore, to obtain higher SL temperatures, we have to produce SL in liquids containing lower partial pressures of heavier noble gases [24].

Appearance of maximization of SL temperature in moderate acid concentrations in low partial pressure of the noble gas proposes this question "does this scenario exist for the acid solutions containing higher amounts of the noble gas too?" To answer this question, we calculated the SL phase diagrams for the acid solutions containing argon at partial pressure of 50 Torr. Then we calculated the maximum SL intensity for each solution and the results have been summarized in Table III together with the results of 4 Torr.

It is seen for the partial pressure of 50 Torr, unlike 4 Torr, there is not any optimum vapor pressure in a moderate acid concentration. In fact, in the case of 50 Torr, both of the SL

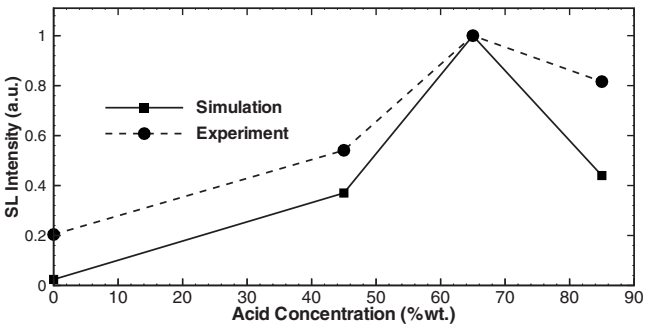

FIG. 3. Comparison of the results of simulation with experimental data of Ref. [18] for maximum SL intensity from different acid solutions. The SL intensities in both simulation and experimental data have been normalized to the maximum SL emission appearing for the solution of 65% acid in both cases.

TABLE IV. The contributions of different phenomena in the change in thermal energy of the SL bubble from the beginning of its oscillation ($t=0$) to the end of collapse. The results are concerned to the conditions of maximum SL emission in different acid solutions. The quantities ΔE_{th}, ΔQ, ΔE_{chem}, and ΔH denote the change in thermal energy, heat, chemical energy, and enthalpy of the bubble, respectively. Also, $W=-\int p_g dv$ is the work done on the bubble during the time $t=0$ to the end of collapse.

Energy change (10^{-10} J)	ΔE_{th}	ΔQ	ΔE_{chem}	ΔH [a]	$W=-\int p_g dv$
		4 Torr			
0% (water)	62.93	−6.03	−2.98	0.00	71.94
45%	185.92	−12.99	−3.52	0.00	202.43
65%	325.33	−19.21	−1.04	0.00	345.58
70%	291.96	−17.77	−0.37	0.00	310.10
85%	241.26	−15.74	−0.01	0.00	257.01
		50 Torr			
0% (water)	23.46	−7.38	−0.01	−0.08	30.93
45%	59.77	−15.88	−0.04	−0.09	75.78
65%	210.77	−46.06	−0.07	−0.05	256.95
70%	380.60	−78.80	−0.07	−0.04	459.51
85%	685.21	−138.20	0.00	0.00	823.42

[a]H is the enthalpy of the bubble defined as $H=\Sigma_j h_{w,j} N_j$.

intensity and the SL temperature monotonically increase with the acid concentration. The difference between the two situations of low and high amounts of the noble gas originates from the difference between them in the amount of bubble expansion and bubble's contents at the collapse. In the case of 4 Torr, the bubble size is relatively small and the pressure amplitude is relatively large. Hence, the ratio of R_{max}/R_0 is large and, consequently, the bubble collapse is violent. Therefore, not only during the bubble expansion a large number of vapor molecules evaporate into the bubble but also at the collapse a less number of them have enough time to be condensed on the bubble interface. In fact, at the end of the collapse, a relatively large number of vapor molecules remain inside the bubble and the presence of these molecules inside the bubble, along with the additional compression produced by the change in the driving parameters of the bubble oscillations, generates the scenario of maximization of SL temperature in a moderate acid concentration.

On the other hand, for the case of 50 Torr, the size of bubble is relatively large (relative to 4 Torr) and, consequently, the bubble expansion and the collapse intensity are weak (compared to 4 Torr). Therefore, there is enough time for vapor molecules to be condensed on the bubble surface during the collapse and the additional compression resulted from the vapor molecules in the bubble of 50 Torr is considerably weaker than that of 4 Torr. This is the main reason that the SL intensity monotonically increases with the acid concentration in 50 Torr. We can see in Table III that in comparison to the case of 4 Torr, both of maximum pressure and maximum number density of the bubble are much smaller in the case of 50 Torr. Moreover, the quantities R_{max}/R_{min} and R_{max}/R_0 are considerably smaller in 50 Torr relative to those of 4 Torr.

It should be mentioned that with the change in the concentration of sulfuric acid, the physical parameters of the liquid surrounding the bubble change. This changes the phase diagrams of the bubble oscillations as well as the driving pressure for the condition of maximum SL radiation. Accordingly, the work done on the bubble by the ultrasound field also changes. For the case of 4 Torr, the work done on the bubble by the external pressure becomes maximum in a moderate acid solution and, consequently, the maximization of SL emission is seen for this solution too.

To clarify the influence of the work of the external pressure on the SL temperature, we have calculated the contribution of different phenomena on the change in the thermal energy of the bubble from the beginning of its oscillation ($t=0$) to the end of the collapse. The results are shown in Table IV. It is seen, in both cases of 4 and 50 Torr, that most of the change in the thermal energy of the bubble comes from the work done by the external ultrasonic field. For 4 Torr, the maximum work done on the bubble appears for the case of 65% acid. For 50 Torr, the work done on the bubble monotonically increases with the acid concentration. The trend of change in the thermal energy of the bubble with the acid concentration is similar to the trend of change in the maximum SL temperature with concentration in Table III.

According to the results of Table IV, the maximization of SL temperature in the solution of 65% acid is originated from the amount of work done on the bubble by the ultrasound field. The work of ultrasound field depends on the driving parameters (P_a and R_0) and these parameters are determined from the stability conditions of the bubble motion. As shown in Table I, among the physical parameters of sulfuric acid, just vapor pressure and viscosity of the liquid considerably change with the acid concentration. For the in-

stability mechanisms of bubble motion, the viscosity and partial pressure of the noble gas are the important parameters determining the ultimate driving conditions. Therefore, the optimum acid concentration corresponding to maximum SL temperature is mainly determined by the change in the viscosity of the acid with concentration and the change in the vapor pressure is less important here.

Since the last few years, several experimental evidences have been proposed indicating the existence of a hot plasma region inside the SL bubble [8–14,33]. This seems to be incompatible with the uniformity assumption used in this work. However, the results of the uniform model can be inferred as the spatial average of the physical characteristics inside the bubble in real state. In fact, what is seen as the experimental SL intensity is almost the spatial average of SL emission from the hot region inside the bubble. Therefore, we expect that as an approximation, the general characteristics of SL radiation and its dependency on the surrounding liquid conditions can be explained by the uniform model. Inevitably, to acquire details of temperature profile inside the bubble, a more complete model, such as a molecular-dynamics description [34,35], is required.

Since most of the experimental researches on sulfuric acid have been performed on concentrated acid solutions, the maximization of SL intensity in moderate acid concentrations has not extensively been explored by experimentalists. For further clarifying this scenario in sulfuric acid and other low vapor pressure liquids, more experimental investigations seem to be necessary.

This work was supported by Tarbiat Modares University (TMU). Financial support by the grant of National Elite Foundation of Iran is gratefully acknowledged.

[1] D. F. Gaitan *et al.*, J. Acoust. Soc. Am. **91**, 3166 (1992).
[2] S. Putterman, Sci. Am. **272**, 46 (1995).
[3] B. Barber *et al.*, Phys. Rep. **281**, 65 (1997).
[4] R. Hiller, S. J. Putterman, and B. P. Barber, Phys. Rev. Lett. **69**, 1182 (1992).
[5] G. Vazquez *et al.*, Opt. Lett. **26**, 575 (2001).
[6] G. Vazquez, C. Camara, S. J. Putterman, and K. Weninger, Phys. Rev. Lett. **88**, 197402 (2002).
[7] C. Camara, S. Putterman, and E. Kirilov, Phys. Rev. Lett. **92**, 124301 (2004).
[8] Y. T. Didenko, W. B. McNamara, III, and K. S. Suslick, Nature (London) **407**, 877 (2000).
[9] J. B. Young, J. A. Nelson, and W. Kang, Phys. Rev. Lett. **86**, 2673 (2001).
[10] D. Flannigan and S. K. Suslick, ARLO **6**, 157 (2005).
[11] D. J. Flannigan and K. S. Suslick, Phys. Rev. Lett. **95**, 044301 (2005).
[12] D. Flannigan and S. K. Suslick, J. Phys. Chem. A **110**, 9315 (2006).
[13] D. Flannigan and S. K. Suslick, Nature (London) **434**, 52 (2005).
[14] Y. Didenko and S. K. Suslick, Nature (London) **418**, 394 (2002).
[15] M. P. Brenner, S. Hilgenfeldt, and D. Lohse, Rev. Mod. Phys. **74**, 425 (2002).
[16] A. Chakravarty, T. Georghiou, T. E. Phillipson, and A. J. Walton, Phys. Rev. E **69**, 066317 (2004).
[17] S. D. Hopkins, S. J. Putterman, B. A. Kappus, K. S. Suslick, and C. G. Camara, Phys. Rev. Lett. **95**, 254301 (2005).
[18] A. Troia, D. Madonna Ripa, and R. Spagnolo, Ultrason. Sonochem. **13**, 278 (2006).
[19] X. Lu, A. Prosperetti, R. Toegel, and D. Lohse, Phys. Rev. E **67**, 056310 (2003).
[20] A. Moshaii and R. Sadighi-Bonabi, Phys. Rev. E **70**, 016304 (2004).
[21] J. B. Keller and M. J. Miksis, J. Acoust. Soc. Am. **68**, 628 (1980).
[22] R. Toegel *et al.*, Phys. Rev. Lett **88**, 034301 (2002).
[23] Y. Ho *et al.*, J. Phys. Chem. Ref. Data **1**, 279 (1972).
[24] A. Moshaii *et al.*, Phys. Lett. A **372**, 1283 (2008).
[25] G. F. Puente, P. Garcia-Martinez, and F. J. Bonetto, Phys. Rev. E **75**, 016314 (2007).
[26] C. Matsuoka and K. Nishihara, Phys. Rev. E **74**, 049902(E) (2006).
[27] S. Fujikawa and T. Akumatsu, J. Fluid Mech. **97**, 481 (1980).
[28] K. Yasui, Phys. Rev. E **56**, 6750 (1997).
[29] L. Gmelin and R. J. Meyer, *Gmelins Handbuch Der Anorganischen Chemie* (Verlag Chemie GmbH, Leipzig, 1985).
[30] NIST, Chemistry Webbook, 2001 (http://webbok.nist.gov/chemistry/).
[31] I. Akhatov, R. Mettin, C. D. Ohl, U. Parlitz, and W. Lauterborn, Phys. Rev. E **55**, 3747 (1997).
[32] K. Yasui, Phys. Rev. E **64**, 016310 (2001).
[33] D. J. Flannigan and K. S. Suslick, Phys. Rev. Lett. **99**, 134301 (2007).
[34] S. J. Ruuth, S. Putterman, and B. Merriman, Phys. Rev. E **66**, 036310 (2002).
[35] A. Bass, S. J. Ruuth, C. Camara, B. Merriman, and S. Putterman, Phys. Rev. Lett. **101**, 234301 (2008).